

## Supporting Information



Figure S1 the fresh preparation of MnO<sub>2</sub> nanosheets and corresponding *Dindal phenomenon*.

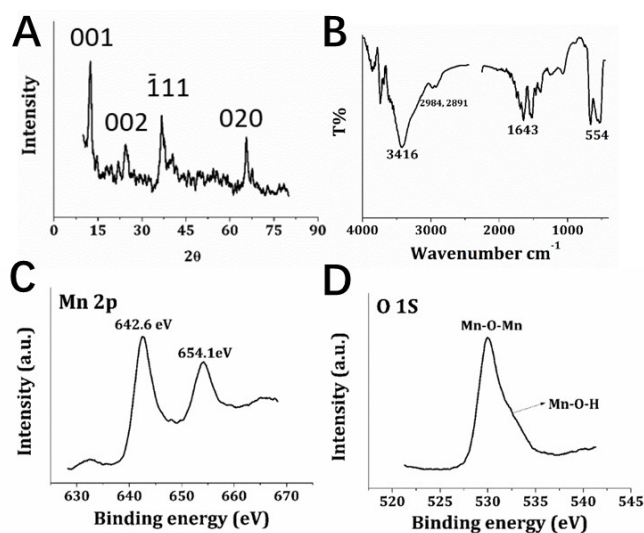


Figure S2 XRD (A) and FTIR (B) of MnO<sub>2</sub> nanosheets; XPS spectrum of MnO<sub>2</sub> nanosheets for Mn 2p (C) and O 1s (D)

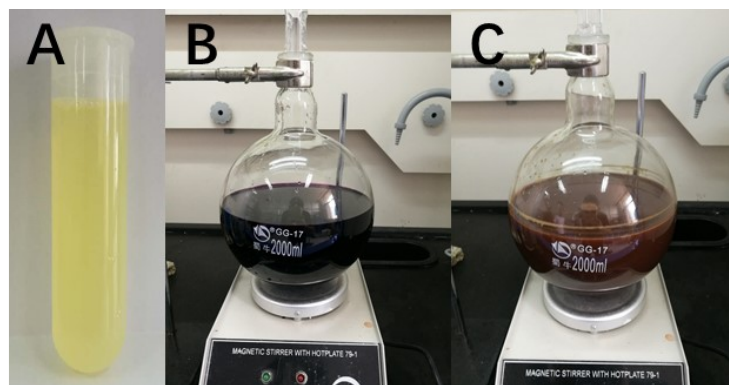


Figure S3 (A) the fresh-squeezing orange juice; large scale preparation of  $\text{MnO}_2$  nanosheets: (B) 1.6 g of  $\text{KMnO}_4$  dissolved in 1.6 L aqueous solution; (C) after reaction with orange juice for 30 minutes

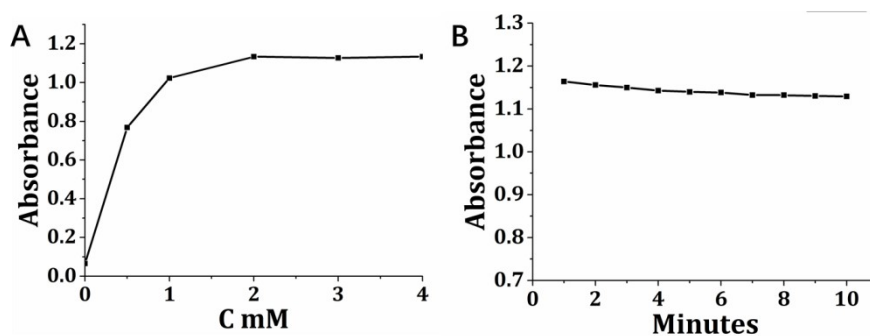


Figure S4 absorbance values of  $\text{MnO}_2$  nanosheets-TMB system with different concentration of TMB (A) and different incubation time (B)

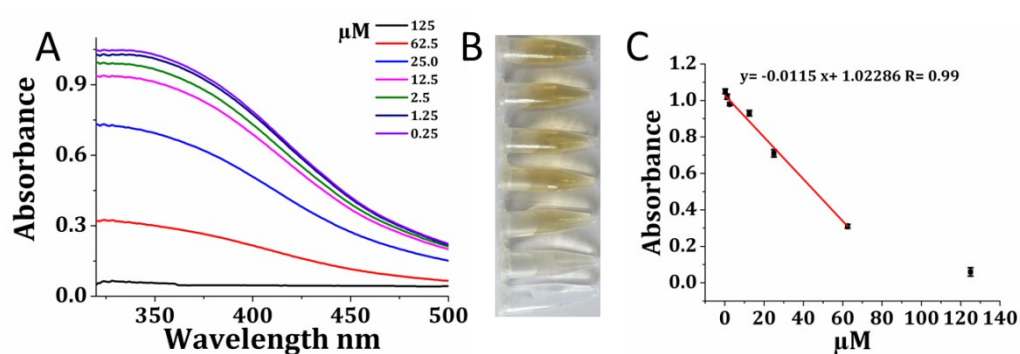


Figure S5 UV-vis absorbance spectrum of  $\text{MnO}_2$  nanosheets incubated with different concentration of GSH from 0.25  $\mu\text{M}$  to 125  $\mu\text{M}$  (A) and corresponding digital

photographs (B); the calibration curve between concentration of GSH and absorbance value at 350 nm

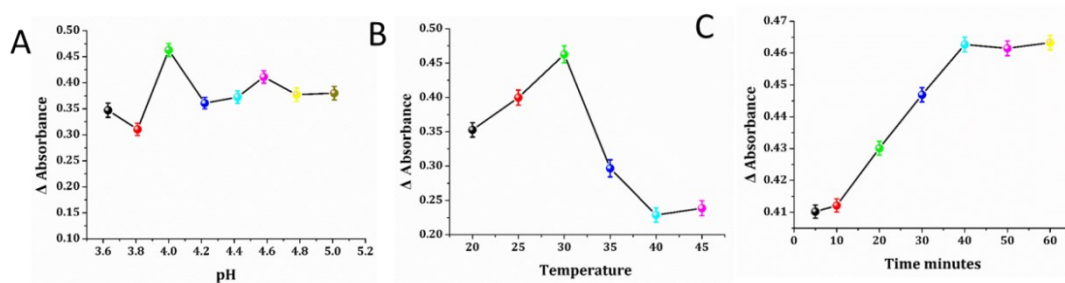


Figure S6 optimizing of buffer pH (A), incubation temperature (B) and time(C)

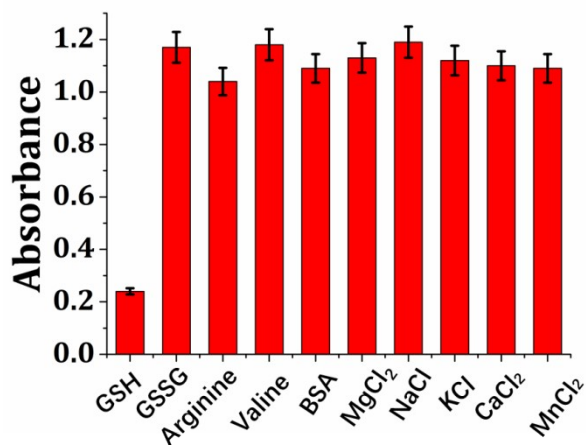


Figure S7 Specificity of  $\text{MnO}_2$  nanosheets-TMB system for biosensing of GSH

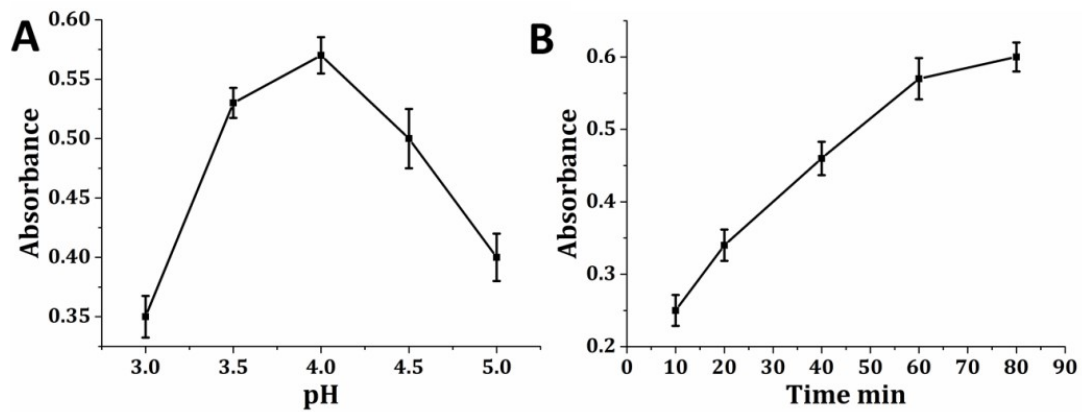


Figure S8 optimizing experimental conditions of the colorimetric immunosensor: (A) pH; (B) incubation time

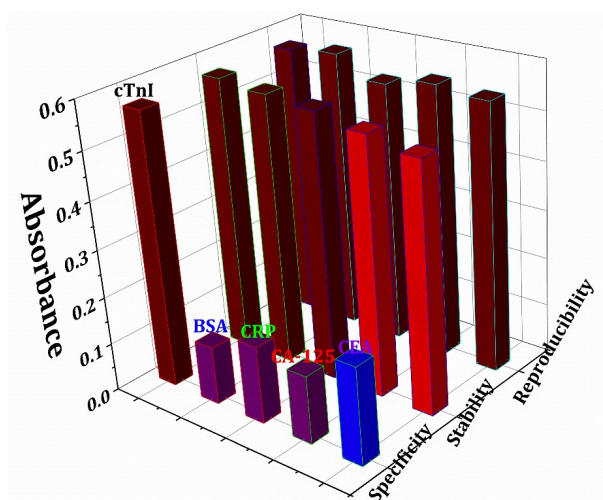


Figure S9 The specificity, stability and reproducibility of colorimetric immunosensor



Figure S10 smartphone-enabled immunoassay of various concentration of cTnI from  $0.001 \text{ ng mL}^{-1}$  to  $10 \text{ ng mL}^{-1}$

Table S1 the comparison of different methods for biosensing of GSH

Method	Material	Detection limit	reference
Colorimetric	Cu/CuO-reduced graphene oxide	32 nM	[1]
Fluorometric	BPQDs@MnO <sub>2</sub>	35 nM	[2]
Magnetic/Fluorometric	Carbon dots/MnO <sub>2</sub>	0.6 $\mu\text{M}$	[3]
Fluorometric	C <sub>3</sub> N <sub>4</sub> /Cu <sup>2+</sup>	20 nM	[4]
Fluorometric	AuNCs@MnO <sub>2</sub>	0.67 $\mu\text{M}$	[5]
Luminescent	MnO <sub>2</sub> /Iridium	0.13 $\mu\text{M}$	[6]
Fluorometric	MnO <sub>2</sub> -Si quantum dots	0.153 $\mu\text{M}$	[7]
Fluorometric	MnO <sub>2</sub> nanosheets/carbon dots	22 nM	[8]

Ratiometric fluorometric	Carbon dots	20 nM	[9]
Colotimetric	MnO <sub>2</sub> nanosheets	0.08 nM	This work

Table S2 the comparison of different methods for biosensing of cTnI

Method	Material	Detection limit	reference
Electrochemical aptasensor	DNA nanotetrahedron	10 pg mL <sup>-1</sup>	[10]
Localize surface plasmon resonance	peptide-modified plasmonic gold nanohole	1.8 ng mL <sup>-1</sup>	[11]
Impedimetric immonosensor	Graphene-multi-walled carbon nanotube	0.94 pg mL <sup>-1</sup>	[12]
Colorimetric	Peptide Functionalized Gold Nanoparticles	0.2 ng mL <sup>-1</sup>	[13]
Electrochemical aptasensor	Aptamer candidates	24 pg mL <sup>-1</sup>	[14]
Electrode biochip	Biofunctionalized Rebar Graphene	1 pg mL <sup>-1</sup>	[15]
Electrochemical biosensors	TdT assisted aptamer	40 pg mL <sup>-1</sup>	[16]
Electrochemical immunosensor	Carbon nanofiber	0.2 ng mL <sup>-1</sup>	[17]
Colorimetric	MnO <sub>2</sub> nanosheets	0.70 pg mL <sup>-1</sup>	This work

## References

- [1] P. Singh, P. Nath, R.K. Arun, S. Mandal, N. Chanda, Novel synthesis of a mixed Cu/CuO–reduced graphene oxide nanocomposite with enhanced peroxidase-like

catalytic activity for easy detection of glutathione in solution and using a paper strip, RSC Advances 6 (2016) 92729-92738.

[2] H. Li, R. Xie, C. Huang, J. He, P. Yang, J. Tao, B. Lin, P. Zhao, Black phosphorus quantum dots nanocomposites based activatable bimodal imaging and determination of intracellular glutathione, Sensors and Actuators B: Chemical 321 (2020) 128518.

[3] Y. Xu, X. Chen, R. Chai, C. Xing, H. Li, X.-B. Yin, A magnetic/fluorometric bimodal sensor based on a carbon dots–MnO<sub>2</sub> platform for glutathione detection, Nanoscale 8 (2016) 13414-13421.

[4] C. Yang, X. Wang, H. Liu, S. Ge, J. Yu, M. Yan, On–off–on fluorescence sensing of glutathione in food samples based on a graphitic carbon nitride (gC<sub>3</sub>N<sub>4</sub>)–Cu<sup>2+</sup> strategy, New J. Chem. 41(2017) 3374-3379.

[5] H. Yao, D. Jiang, G. Dong, J. Sun, S. Sun, L. Li, F. Zheng, W. Xiong, Near infrared imaging of intracellular GSH by AuNCs@MnO<sub>2</sub> core-shell nanoparticles based on the absorption competition mechanism, Analyst 146 (2021) 5115-5123.

[6] Z.-Z. Dong, L. Lu, C.-N. Ko, C. Yang, S. Li, M.-Y. Lee, C.-H. Leung, D.-L. Ma, A MnO<sub>2</sub> nanosheet-assisted GSH detection platform using an iridium (iii) complex as a switch-on luminescent probe, Nanoscale 9(2017) 4677-4682.

[7] H. Ma, X. Li, X. Liu, M. Deng, X. Wang, A. Iqbal, W. Liu, W. Qin, Fluorescent glutathione probe based on MnO<sub>2</sub>–Si quantum dots nanocomposite directly used for

intracellular glutathione imaging, *Sensors and Actuators B: Chemical* 255 (2018) 1687-1693.

[8] Y. Wang, K. Jiang, J. Zhu, L. Zhang, H. Lin, A FRET-based carbon dot–MnO<sub>2</sub> nanosheet architecture for glutathione sensing in human whole blood samples, *Chem. Commun.* 51 (2015) 12748-12751.

[9] S. Lu, D. Wu, G. Li, Z. Lv, Z. Chen, L. Chen, G. Chen, L. Xia, J. You, Y. Wu, Carbon dots-based ratiometric nanosensor for highly sensitive and selective detection of mercury (II) ions and glutathione, *RSC Advances* 6 (2016) 103169-103177.

[10] D. Sun, Z. Luo, J. Lu, S. Zhang, T. Che, Z. Chen, L. Zhang, Electrochemical dual-aptamer-based biosensor for nonenzymatic detection of cardiac troponin I by nanohybrid electrocatalysts labeling combined with DNA nanotetrahedron structure, *Biosensors and Bioelectronics* 134 (2019) 49-56.

[11] J. Zhang, Y. Wang, T.I. Wong, X. Liu, X. Zhou, B. Liedberg, Electrofocusing-enhanced localized surface plasmon resonance biosensors, *Nanoscale* 7(2015) 17244-17248.

[12] S. Singal, A.K. Srivastava, S. Dhakate, A.M. Biradar, Electroactive graphene-multi-walled carbon nanotube hybrid supported impedimetric immunosensor for the detection of human cardiac troponin-I, *Rsc Advances* 5 (2015) 74994-75003.

[13] X. Liu, Y. Wang, P. Chen, A. McCadden, A. Palaniappan, J. Zhang, B. Liedberg, Peptide functionalized gold nanoparticles with optimized particle size and



concentration for colorimetric assay development: Detection of cardiac troponin I, *Acs Sensors* 1(2016) 1416-1422.

[14] H. Jo, H. Gu, W. Jeon, H. Youn, J. Her, S.-K. Kim, J. Lee, J.H. Shin, C. Ban, Electrochemical aptasensor of cardiac troponin I for the early diagnosis of acute myocardial infarction, *Anal. Chem.* 87 (2015) 9869-9875.

[15] S.K. Tuteja, P. Sabherwal, A. Deep, R. Rastogi, A.K. Paul, C.R. Suri, Biofunctionalized rebar graphene (f-RG) for label-free detection of cardiac marker troponin I, *ACS applied materials & interfaces* 6 (2014) 14767-14771.

[16] M. Lang, D. Luo, G. Yang, Q. Mei, G. Feng, Y. Yang, Z. Liu, Q. Chen, L. Wu, An ultrasensitive electrochemical sensing platform for the detection of cTnI based on aptamer recognition and signal amplification assisted by TdT, *RSC Adv* 10 (2020) 36396-36403.

[17] A. Periyakaruppan, R.P. Gandhiraman, M. Meyyappan, J.E. Koehne, Label-free detection of cardiac troponin-I using carbon nanofiber based nanoelectrode arrays, *Anal. Chem.* 85 (2013) 3858-3863.